Supporting Information

Reactivity and stability synergism directed by the electron transfer between polyoxometalates and metal−organic frameworks

Xinlin Lu, Ting Cheng, Yurii V. Geletii*, John Bacsa, and Craig L. Hill*

Department of Chemistry, Emory University, Atlanta, GA 30322

Corresponding Authors

iguelet@emory.edu; chill@emory.edu

General Methods and Materials

All the polyoxometalates (POM) including $[PVMo_{11}]^{4-}$, $[PV_2Mo_{10}]^{5-}$, $[PV_3Mo_9]^{6-}$, $[PVW_{11}]^{5-}$, $[PV_2W10]^{5-}$, $[PCoW_{11}]^{5-}$, $[PNiW_{11}]^{5-}$ and $[PCuW_{11}]^{5-}$ were synthesized according to literature methods.[1–6] **PVMo**@HKUST ($PV_nMo_{12-n}O_{40}^{(3+n)-}$) $[PMo_{12}]^{3-}$, $[PVMo_{11}]^{4-}$, $[PV_2Mo_{10}]^{5-}$ and $[PV_3Mo_9]^{6-}$, in HKUST-1) and **PW$_{12}$**@HKUST were prepared following literature methods.[7,8] All other chemicals and solvents were purchased from commercial sources without further purification. The FT-IR spectra were collected on a Nicolet TM 600 FT-IR spectrometer by the attenuated total reflectance (ATR) sampling technique. Powder XRD data were collected on a D8 Discover Powder Instrument using monochromatic Cu Kα (λ = 1.54060 Å) radiation. The single crystal XRD data were collected either on a Bruker D8 SMART APEX CCD or on a Rigaku Synergy-S diffractometer using Mo Kα (0.71073 Å) or Cu Kα (λ = 1.54060 Å) radiation. SEM-EDX data were collected on a HITACHI SU8230 FE-SEM. The POM@MOF samples were coated with gold using a Hummer 6 sputterer. UV−vis spectra were collected with an Agilent 8453 spectrophotometer using a 1.0 cm optical path length quartz cuvette. The kinetics were followed by an SF-61 stopped-flow instrument (Hi-Tech Scientific, U.K.) ^{1}H nuclear magnetic resonance (NMR) spectra were acquired on a Varian INOVA 400 spectrometer. The thermogravimetric (TGA) data were collected on a Mettler Toledo TGA instrument. X-ray photoelectron spectroscopy (XPS) was conducted on a thermos K-ALPHA XPS instrument. The nitrogen isotherms were collected by Micromeritics Instrument Corporation.

Synthesis of POM@HKUST

PXW@HKUST ($[PVW_{11}]^{5-}$, $[PCoW_{11}]^{5-}$ and $[PNiW_{11}]^{5-}$ in HKUST-1) were synthesized by modified methods as previously reported for **PCuW$_{11}$**@HKUST.[9] In a typical experiment,

$Cu(NO_3)_2 \cdot 2.5H_2O$ (240 mg) and POM (200 mg) were added to a flask with 10 mL of distilled water and stirred for 20 min. Trimesic acid (210 mg) and $(CH_3)_4NOH$ (180 mg) were then added sequentially and stirred for 10 min after each addition. The solution was stirred until a uniform dispersion was achieved. The resulting solution (pH ~ 2 for $[PVW_{11}]^{5-}$, pH ~ 4 for $[PCoW_{11}]^{5-}$ and $[PNiW_{11}]^{5-}$) was transferred to a Teflon-lined Parr bomb, programmatically heated up to 200 °C for 16 h, then cooled down and maintained at 100 °C for another 4 h. Finally, the reactor was allowed to cool to ambient temperature. Blue or dark green crystals were obtained and separated from the solution. The products were washed 3 times with distilled water, 3 times with 50% v/v ethanol at 50 °C, then dried in vacuo overnight to remove solvent molecules. The crystal structures were characterized by single crystal X-ray diffraction. Their purity was confirmed by Fourier transform infrared (FT-IR) and powder X-ray diffraction (XRD) analyses. The new materials in this work are **PVW$_{11}$@HKUST**, **PCoW$_{11}$@HKUST** and **PNiW$_{11}$@HKUST**.

The number of TMA counterions and water molecules were estimated by TGA (Figure S23), and their empirical formula are given as: $[Cu_3(C_9H_3O_6)_2]_4[\{(CH_3)_4N\}_4PVW_{11}O_{40}] \cdot 27H_2O$ (**PVW$_{11}$@HKUST**), $[Cu_3(C_9H_3O_6)_2]_4[\{(CH_3)_4N\}_5PCoW_{11}O_{39}] \cdot 27H_2O$ (**PCoW$_{11}$@HKUST**), $[Cu_3(C_9H_3O_6)_2]_4[\{(CH_3)_4N\}_5PNiW_{11}O_{39}] \cdot 27H_2O.$ (**PNiW$_{11}$@HKUST**), $[Cu_3(C_9H_3O_6)_2]_4[\{(CH_3)_4N\}_4PVMo_{11}O_{40}] \cdot 27H_2O$ (**PVMo$_{11}$@HKUST**), $[Cu_3(C_9H_3O_6)_2]_4[\{(CH_3)_4N\}_5PV_2Mo_{10}O_{40}] \cdot 28H_2O$ (**PV$_2$Mo$_{10}$@HKUST**), and $(Cu_3(C_9H_3O_6)_2]_4[\{(CH_3)_4N\}_5HPV_3Mo_9O_{40}) \cdot 27H_2O$ (**PV$_3$Mo$_9$@HKUST**).

Synthesis of POM@MIL-101. The synthesis of POM@MIL-101 materials followed the literature procedure.[10] In a typical synthesis, tetramethylammonium hydroxide (TMAH, 0.043 g) was dissolved in deionized water (5 ml). Then, terephthalic acid (0.166 g) was added and stirred at room temperature for 10 min. Then $[Cr(NO_3)_3] \cdot 9H_2O$ (0.4 g) was added to the mixture resulting in a dark blue suspension with a pH of 2.58. POM (0.2 g) was subsequently added to the solution and stirred for 20 min. The suspension was transferred to a Teflon-lined Parr bomb and kept in an oven at 180 °C for 72 h. The resulting POM@MIL-101 was separated and washed with water and methanol then dried under vacuum overnight.

Single crystal XRD

X-ray Experimental: The material crystallized during hydrothermal synthesis. Data for **PV$_2$Mo$_{10}$@HKUST** were collected from a single crystal at 106(9) K on a XtaLAB Synergy, Dualflex, HyPix four-circle diffractometer with a micro-focus sealed X-ray tube using a mirror as

monochromator and a HyPix detector. The diffractometer was equipped with an Oxford Cryostream 800 low temperature device and used Cu K_α radiation (λ = 1.54184 Å). All data were integrated with CrysAlisPro and a gaussian absorption correction using SCALE3 ABSPACK was applied.[11, 12] The structure was solved by dual methods with SHELXT and refined by full-matrix least-squares methods against F^2 using SHELXL.[13,14] All non-hydrogen atoms were refined with anisotropic displacement parameters. The hydrogen atoms were refined isotropically on calculated positions using a riding model with their U_{iso} values constrained to 1.5 times the U_{eq} of their pivot atoms for terminal sp^3 carbon atoms and 1.2 times for all other carbon atoms

Structure Solution: The structure solution from ShelxT of the PV_2Mo_{10} structure of **PV_2Mo_{10}@HKUST** was found to be chiral and from this preliminary structure with 23 symmetry, we identified a Keggin that contained a PV_2Mo_{10} group with the atoms being partially resolved. The Mo atom is lifted off its mean position by static disorder. It could be modeled by splitting it into two parts and assigning the second part to the V atoms. We refined the site fractions and the positions of the two parts giving a 5:1 ratio for the Mo and V atoms.

For this structural model of PV_2Mo_{10} in F23, there are two whole PV_2Mo_{10} molecules with the V atoms distributed equally among the 12 metal atom sites. There are two components to the disorder (i.e., two groups of atoms), but the ligands (the O atoms) were not split, due to the complexity of the model. The elongated ellipsoids can be thought of instead as representing the two unique M-O groups of bonds (with one PO_4 tetrahedron). The distortions and geometries of the ligands were straightforward to analyze once this was done. This partially resolved PV_2Mo_{10} anion was found to be packed into the pores of HKUST-1, with the terminal oxygen pointing towards the di-copper nodes. Furthermore, the crystals were found to be racemically twinned, which may be why the Keggin structure had resolved. Each twin domain contained only one enantiomer, but due to the 50% twinning, the crystal had equal proportions of domains with each enantiomer. We determined that PV_3Mo_9@HKUST is also chiral and isostructural with PV_2Mo_{10}@HKUST.

Thiol (RSH) oxidation

An exemplary substrate, 2-mercaptoethanol, was used for probing the aerobic thiol oxidation mechanism, eq S1, where RSH is 2-mercaptoethanol. The product (bis(2-hydroxyethyl) disulfide (RSSR)) was formed.

$$2\ RSH + \tfrac{1}{2}\ O_2 \rightarrow RSSR + H_2O \qquad\qquad (S1)$$
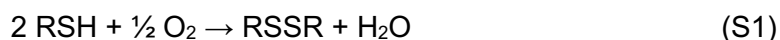
In a typical RSH oxidation catalyzed by the heterogeneous POM@HKUST systems, 20 mg catalyst, 28.6 mM RSH and 5 mL dichloroethane were stirred in a 50 mL heavy-wall glass pressure vessel at 50 °C under air. Aliquots were withdrawn every hour, and the RSH concentration was determined using Ellman's reagent, 5,5-dithiobis(2-nitrobenzoic acid (DTNB).[11] The head space of the vessel was purged with fresh air every hour. The product RSSR was confirmed by ^1H NMR (Figure S25). The POM@HKUST catalysts were collected by centrifugation and dried under vacuum overnight then evaluated to quantify stability. The IR spectrum and powder XRD were measured and compared with those data before RSH oxidation. Reaction kinetics were followed by UV-vis spectroscopy or stopped-flow spectroscopy and described previously.[12]

Electrochemistry

Electrochemical data were obtained using a Pine WaveDiver 10 potentiostat. Cyclic voltammograms (CVs) were recorded in a standard three-electrode electrochemical cell with a glassy carbon disk working electrode, a platinum wire counter electrode, an Ag/AgCl (3M KCl) reference electrode and 0.1 M KNO_3 as the supporting electrolyte. For heterogeneous POM@MOF materials, CVs were collected by immobilizing them on glassy carbon electrode. The measured potential was converted to the reversible hydrogen electrode (RHE). For bulk electrolysis, a reticulated vitreous carbon working electrode was used as a working electrode. UV-vis spectra of the aliquots that after bulk electrolysis at desired constant potential were collected under Ar.
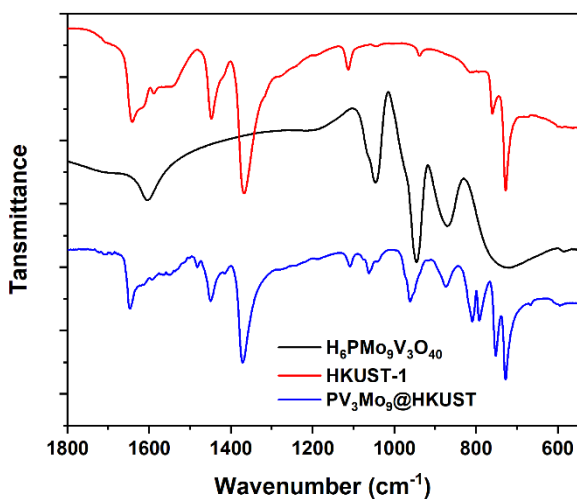
(a)
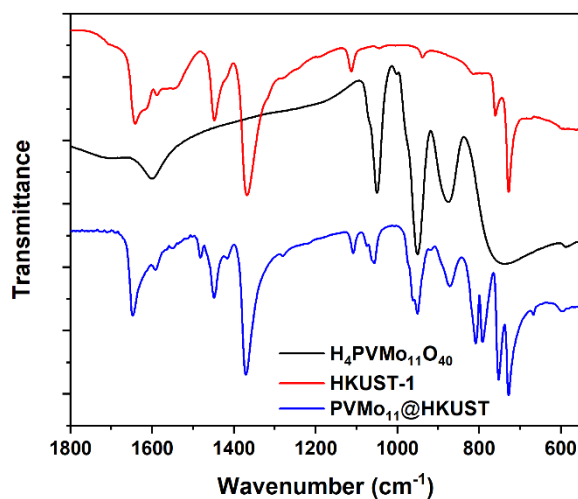
(b)
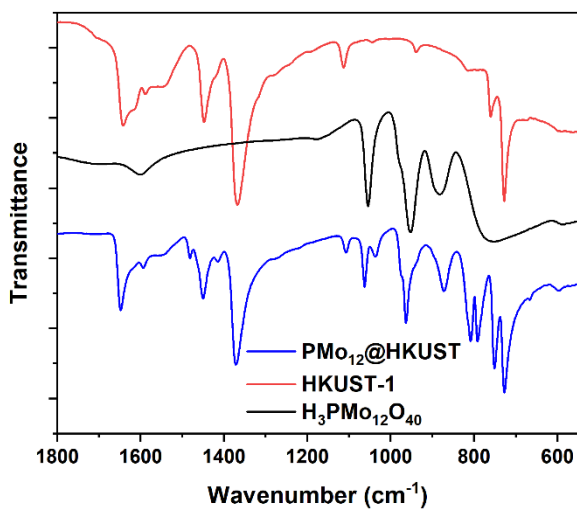
(c)

Figure S1. FT-IR of POM, HKUST-1 and corresponding POM@HKUST (a) **PMo$_{12}$**@HKUST; (b) **PVMo$_{11}$**@HKUST; (c) **PV$_3$Mo$_9$**@HKUST.
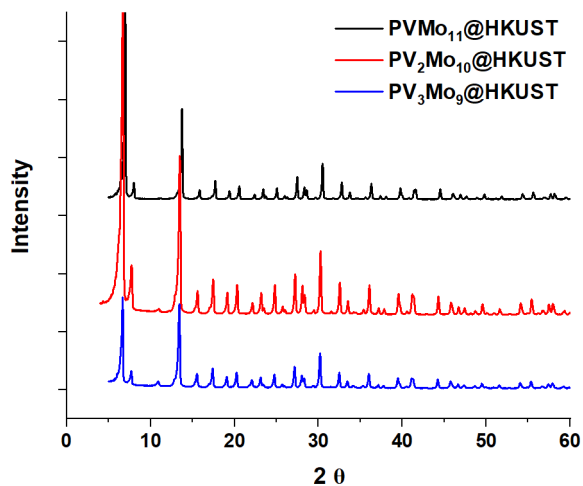
Figure S2. Powder XRD pattern of **PVMo$_{11}$@HKUST**, **PV$_2$Mo$_{10}$@HKUST** and **PV$_3$Mo$_9$@HKUST**.
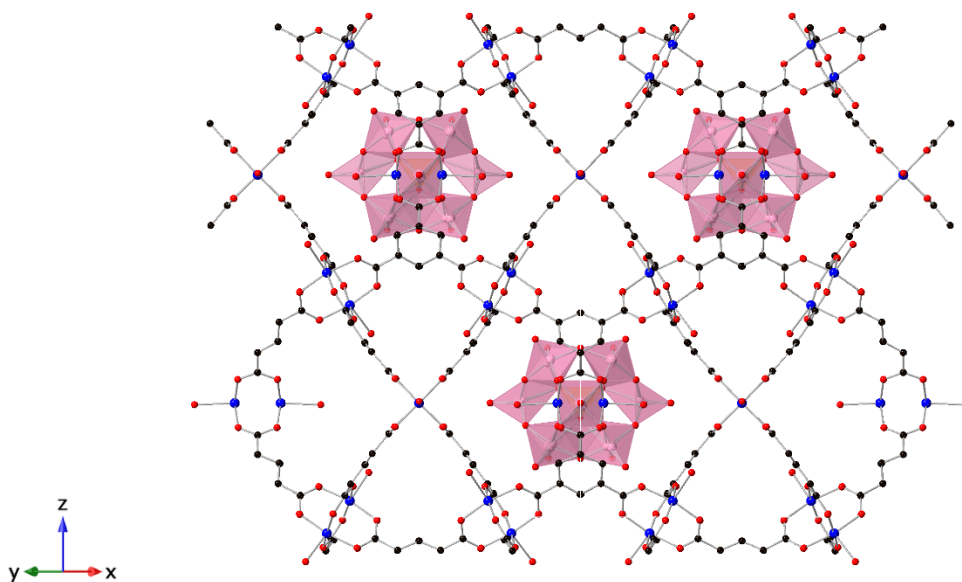

Figure S3. X-ray single-crystal structure of **PV$_2$Mo$_{10}$@HKUST** [110] direction. The purple polyhedral represent the MoO$_6$ (or VO$_6$) and orange tetrahedra represent the PO$_4$ units in the POM. The HKUST-1 framework is represented in ball-and-stick form. C is black, O is red, Cu is blue.

Table S1. Crystal data and structure refinement for PV$_2$Mo$_{10}$@HKUST

CCDC number	
Empirical formula	C$_{92}$H$_{108}$Cu$_{12}$Mo$_{10}$N$_5$O$_{116}$PV$_2$
Formula weight	4994.56
Temperature [K]	106(9)
Crystal system	cubic
Space group (number)	F23 (196)
a [Å]	26.2487(4)
b [Å]	26.2487(4)
c [Å]	26.2487(4)
α [°]	90
β [°]	90
γ [°]	90
Volume [Å^3]	18085.2(8)
Z	4
ρ_{calc} [gcm^{-3}]	1.834
μ [mm^{-1}]	8.780
F(000)	9808
Crystal size [mm^3]	0.07×0.09×0.14
Crystal colour	dark green
Crystal shape	prism
Radiation	Cu K_α (λ=1.54184 Å)
2θ range [°]	5.83 to 152.97 (0.79 Å)
Index ranges	−25 ≤ h ≤ 25
	−32 ≤ k ≤ 32
	−28 ≤ l ≤ 16
Reflections collected	10093
Independent reflections	2902
	R_{int} = 0.0321
	R_{sigma} = 0.0268
Completeness to θ = 67.684°	98.8 %
Data / Restraints / Parameters	2902 / 182 / 179
Goodness-of-fit on F^2	1.074
Final R indexes [I≥2σ(I)]	R_1 = 0.0552
	wR_2 = 0.1605
Final R indexes [all data]	R_1 = 0.0619
	wR_2 = 0.1682
Largest peak/hole [eÅ^{-3}]	0.82/−0.75
Flack X parameter	0.49(4)
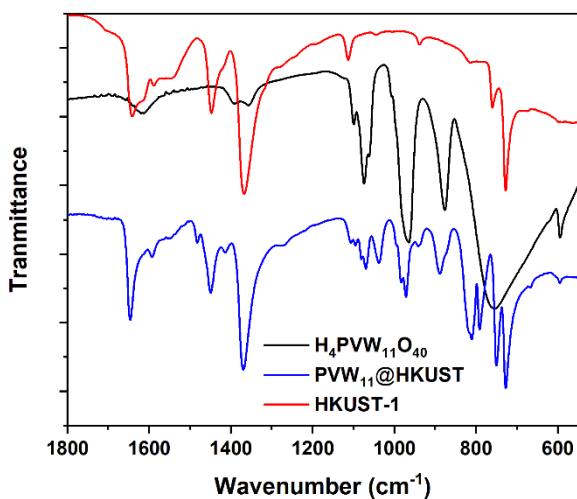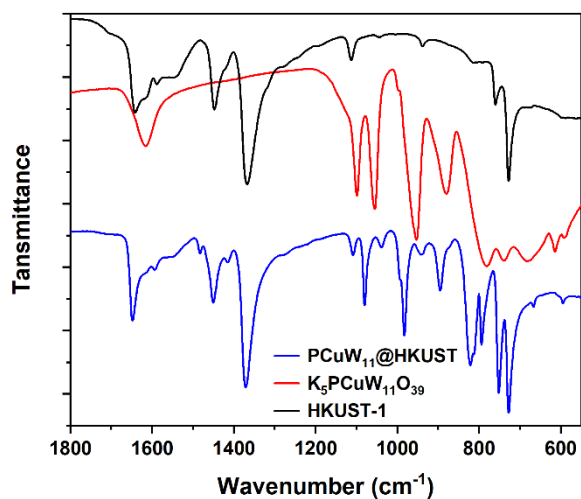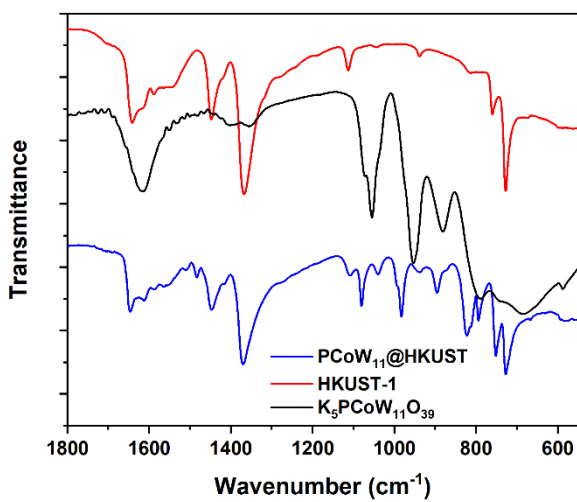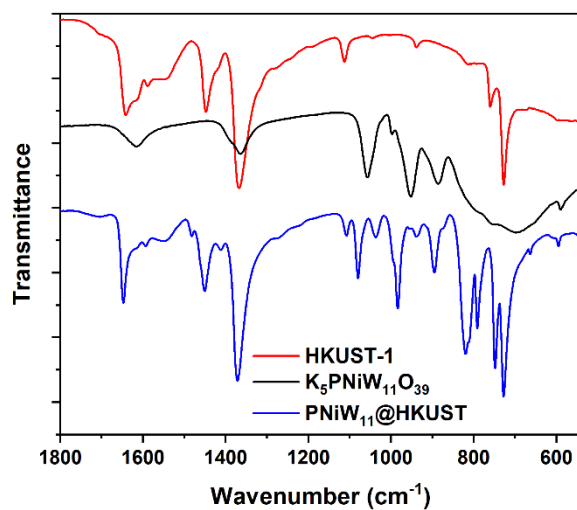
Figure S4. FT-IR of POM alone, HKUST-1 and the corresponding **PXW$_{11}$@HKUST**. (a) **PVW$_{11}$@HKUST**; (b) **PCuW$_{11}$@HKUST**; (c) **PCoW$_{11}$@HKUST**; (d) **PNiW$_{11}$@HKUST**.
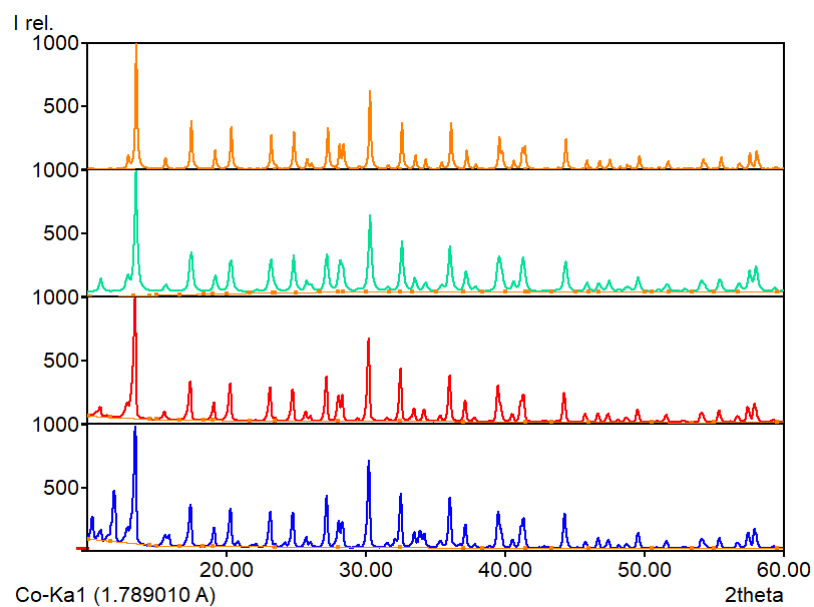
Figure S5. Powder XRD patterns of **PCoW$_{11}$@HKUST**, blue; **PNiW$_{11}$@HKUST**, red; **PVW$_{11}$@HKUST**, green. The calculated pattern from single crystal data of **PCuW$_{11}$@HKUST** is in orange.
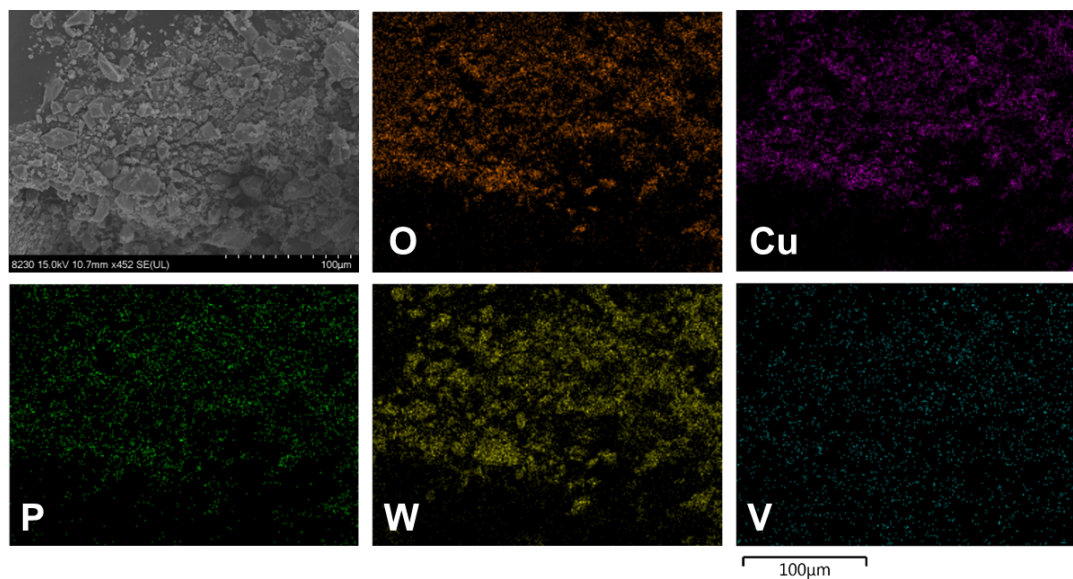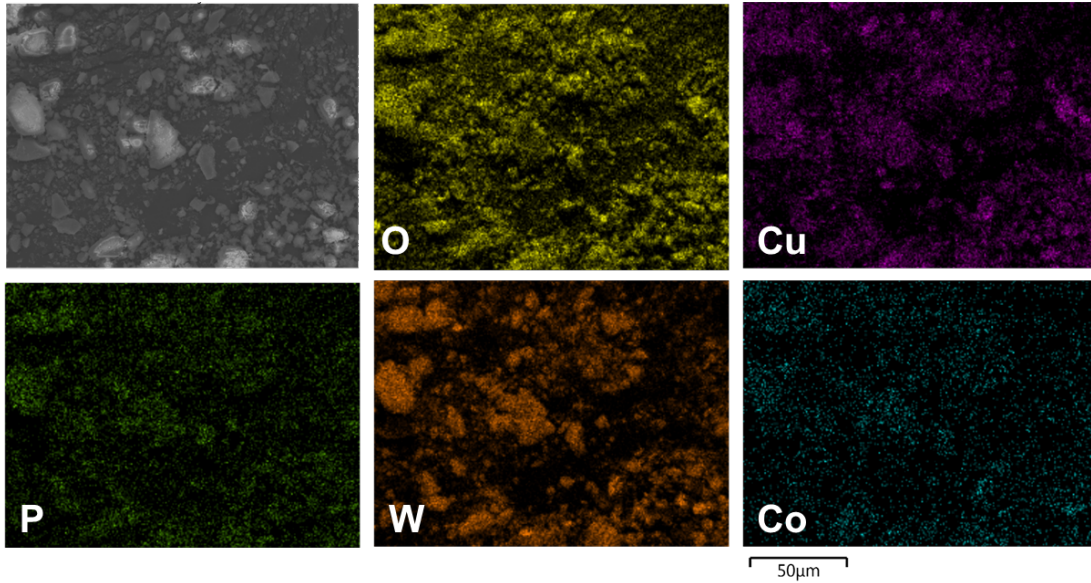

Figure S6. PVW$_{11}$@HKUST SEM image and EDX element mapping.

Figure S7. PCoW₁₁@HKUST SEM image and EDX element mapping.
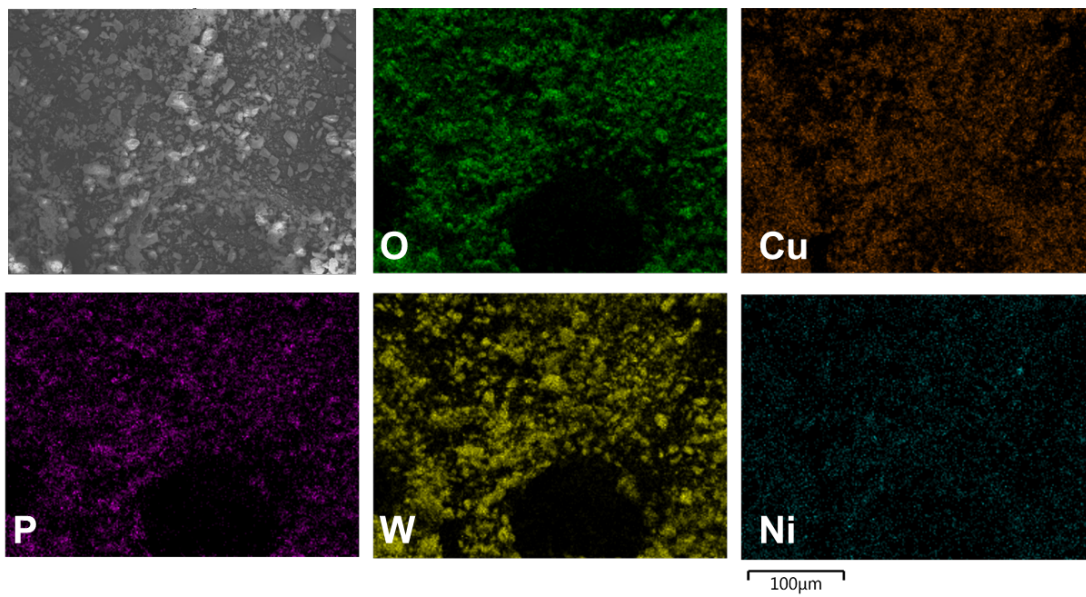
Figure S8. PNiW₁₁@HKUST SEM image and EDX element mapping.
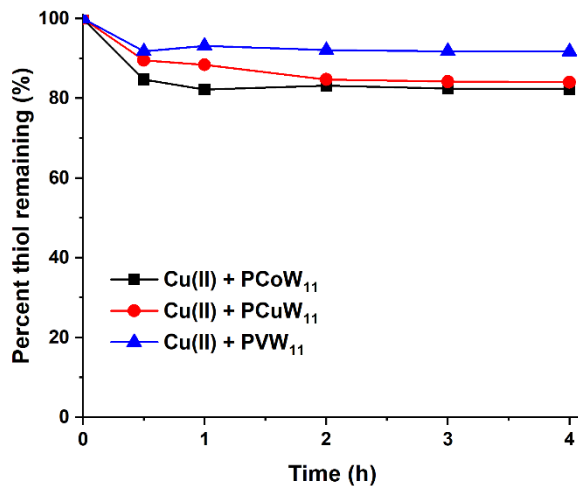
Figure S9. RSH (30 mM) activity catalyzed by 0.2 mM POM with 1.0 mM Cu(II) at room temperature in mixture of dichloroethane with 30%(v/v) acetonitrile. Black: $Na_5PCoW_{11}O_{39}$ (**PCoW_{11}**); Red: $Na_5PCuW_{11}O_{39}$ (**PCuW_{11}**); Blue: $H_5PVW_{11}O_{40}$ (**PVW_{11}**).
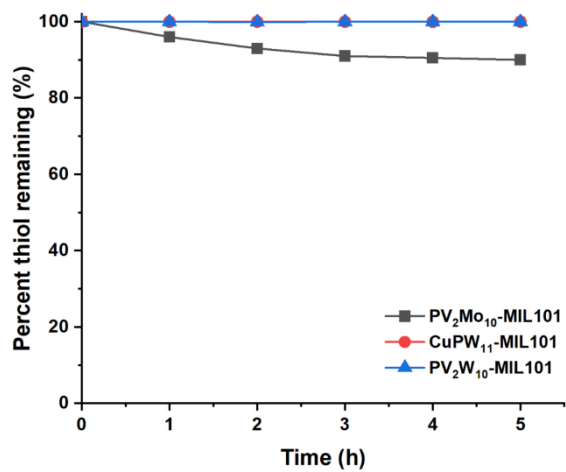
Figure S10. POM@MIL101-catalyzed RSH oxidation activity. Conditions: catalyst (20 mg), 2-mercaptoethanol, RSH (30 mM), dichloroethane (5 mL), at 50 °C under air.

Table S2: Air-based oxidation of 2-mercaptoethanol catalyzed by different POM@HKUST systems[a]

	Conversion[b] %	TON[c], mol g^{-1}	TOF×10^4, mol g^{-1} s^{-1} [d]
HKUST-1	45	0.64	0.089
PMo$_{12}$@HKUST	90	1.16	0.161
PVMo$_{11}$@HKUST	>99	1.43	0.265
PV$_2$Mo$_{10}$@HKUST	>99	1.43	0.662
PV$_3$Mo$_9$@HKUST	>99	1.43	1.324
PCuW$_{11}$@HKUST	63	0.78	0.108
PCoW$_{11}$@HKUST	75	0.93	0.129
PNiW$_{11}$@HKUST	71	0.88	0.122
PVW$_{11}$@HKUST	68	0.84	0.117

[a] Conditions: POM@HKUST (20 mg for **PVMo**@HKUST and 23 mg for **PXW**@HKUST), 2-mercaptoethanol (28.6 mM), dichloroethane (5 mL), at 50 °C under air. [b] Conversion was measured at 20 h. [c] Turnover number (TON = moles of 2-mercaptoethanol consumed per gram of POM@HKUST). TON was measured 15h, 6h and 3h for **PVMo$_{11}$**@HKUST, **PV$_2$Mo$_{10}$**@HKUST and **PV$_3$Mo$_9$**@HKUST respectively. TON was measured at 20h for all the other catalysts. [d] Turnover Frequency, TOF = TON/(reaction time).
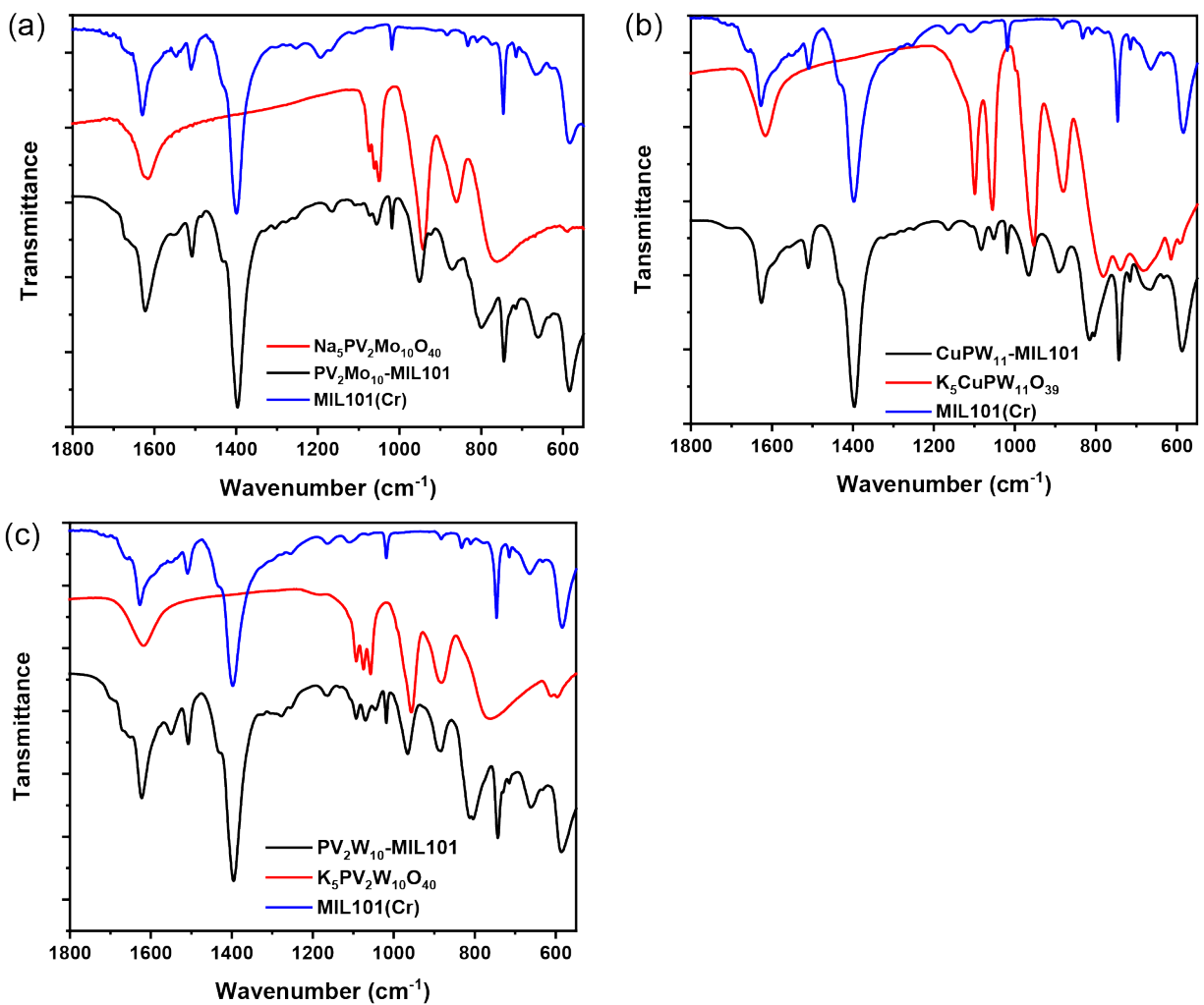
Figure S11. FT-IR of POM, MIL-101(Cr) and corresponding POM@MIL-101 materials: (a) **PV₂Mo₁₀**@MIL-101; (b) **PCuW₁₁**@MIL-101; (c) **PV₂W₁₀**@MIL-101.
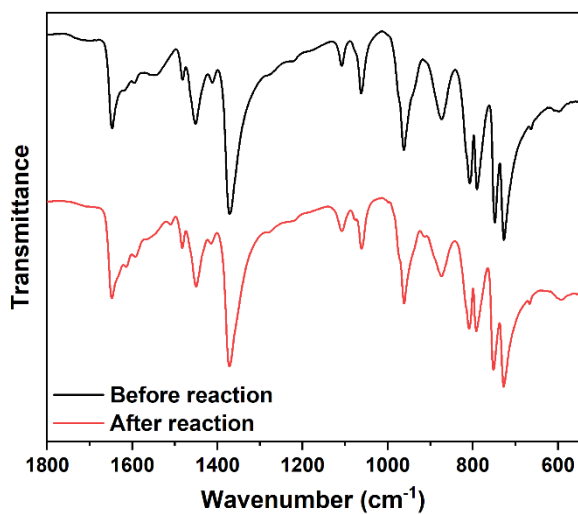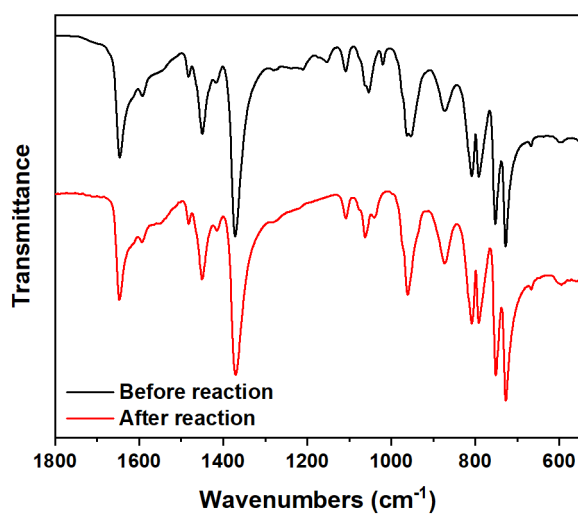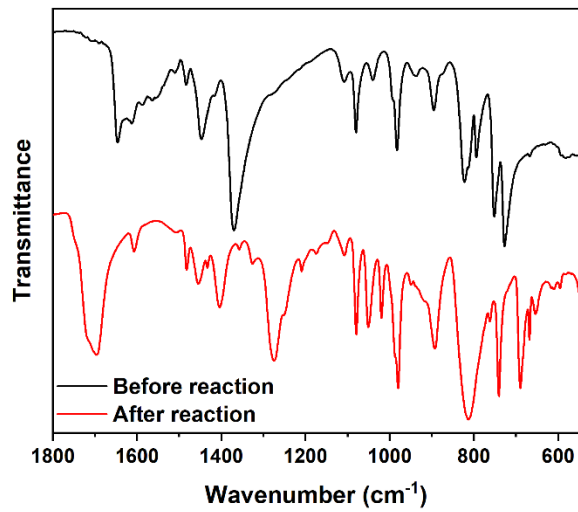
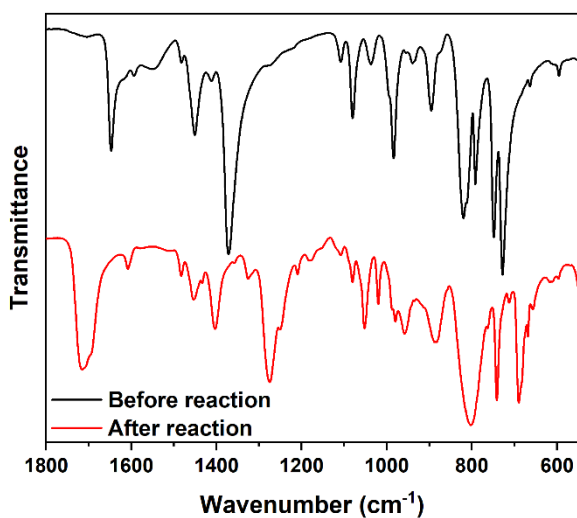**Figure S12.** FT-IR of (a) **PVMo₁₁@HKUST** and (b) **PV₂Mo₁₀@HKUST** before and after RSH oxidation.
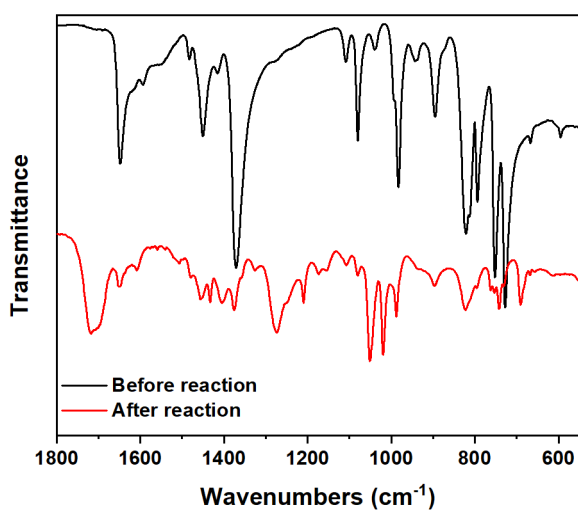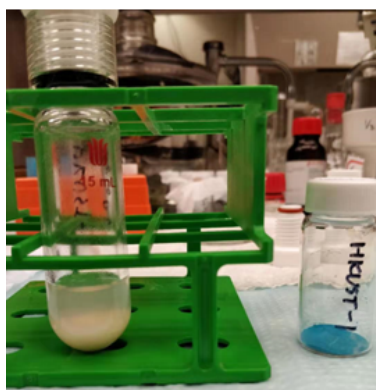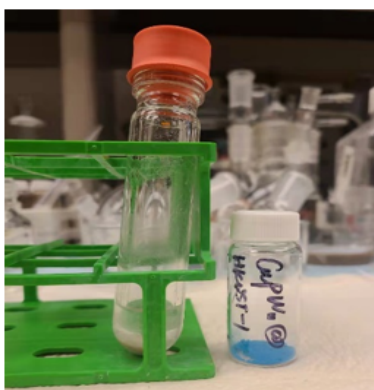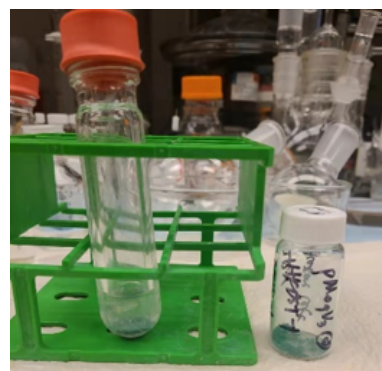
(c)

Figure S13. FT-IR POM@HKUST before and after RSH oxidation. (a) **PCuW₁₁@HKUST**; (b) **PCoW₁₁@HKUST**; (c) **PNiW₁₁@HKUST**.

(a)　　　　　　　　　　(b)　　　　　　　　　　(c)

Figure S14. Digital picture of catalysts before (vials) and after reaction (heavy wall glass pressure vessels). (a) HKUST-1 before reaction is blue crystals; after reaction is white solid. (b) **PCuW₁₁@HKUST** before reaction is blue crystals; after reaction is white solid. (c) **PV₃Mo₉@HKUST** remains green crystals after reaction.
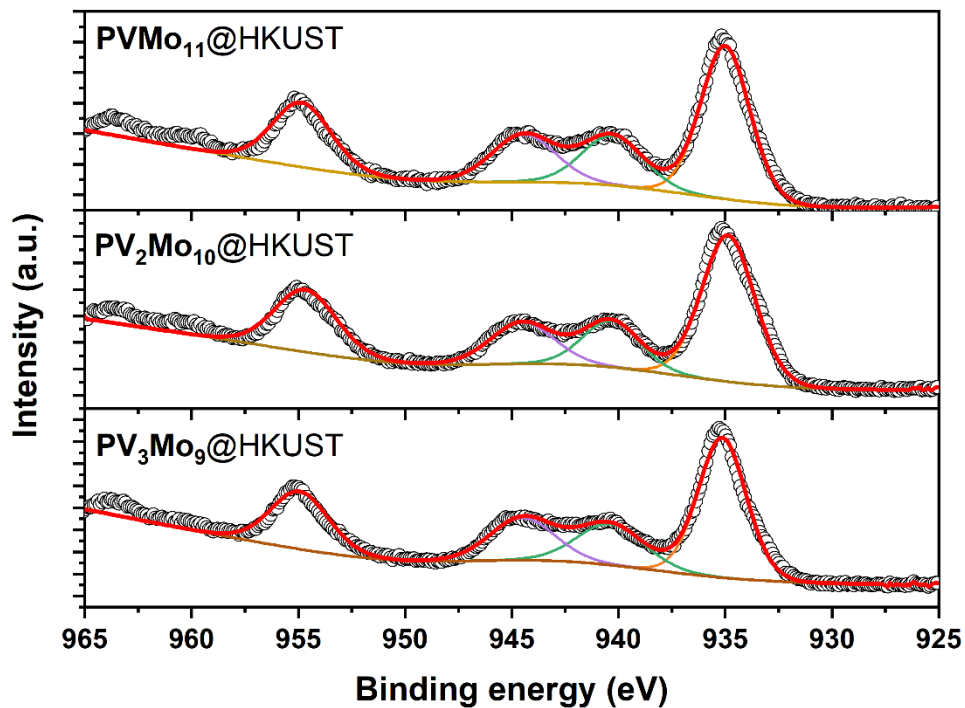
Figure S15. Cu 2p XPS spectra of **PVMo**@HKUST (n= 0-3).
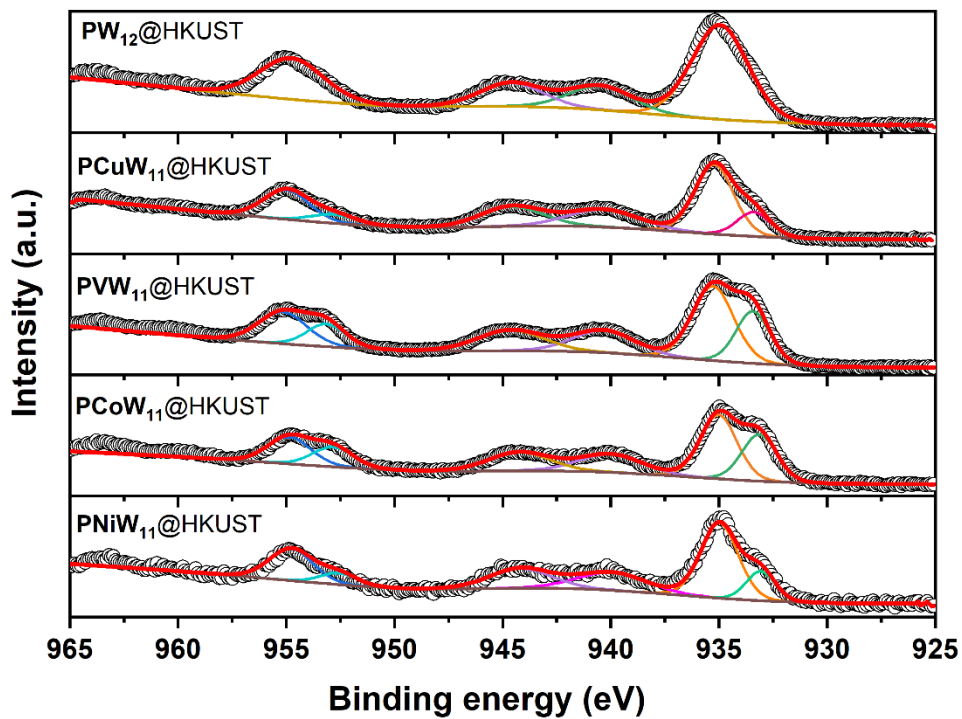
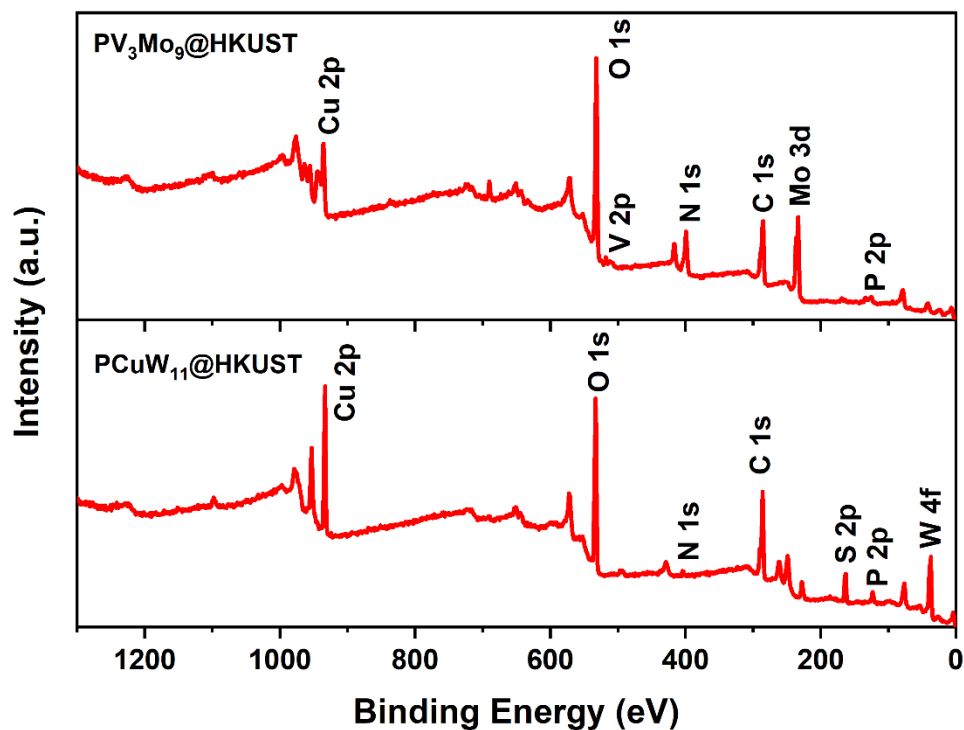**Figure S16.** Cu 2p XPS spectra of **PXW**@HKUST (X = Cu, V, Co and Ni)

Figure S17. XPS survey spectra of **PV₃Mo₉**@HKUST and **PCuW₁₁**@HKUST after RSH oxidation.

Table S3: XPS survey peak table of **PCuW₁₁**@HKUST after RSH oxidation

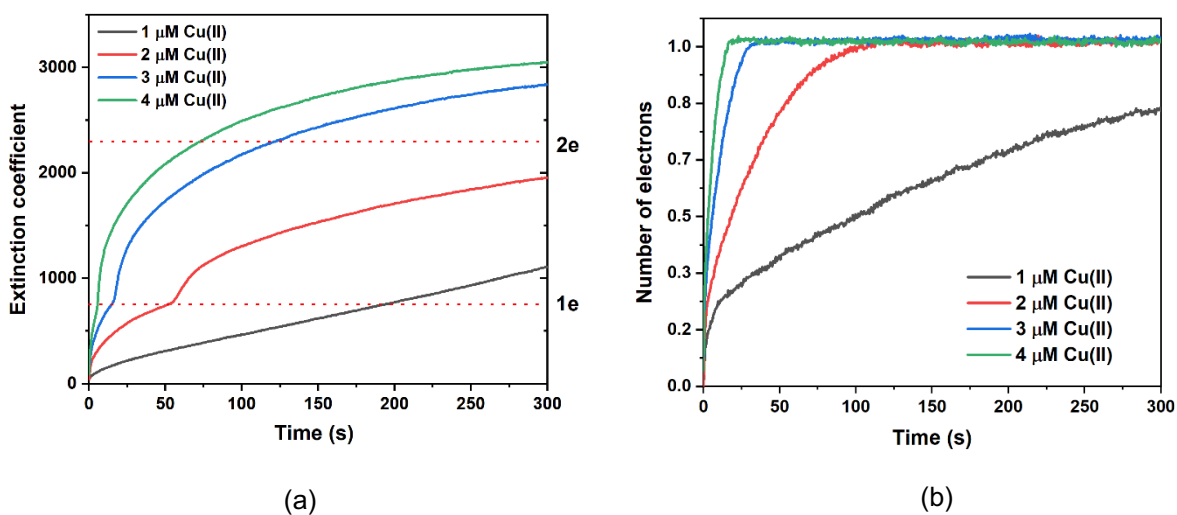| Name	Start BE	Peak BE	End BE	Height CPS	FWHM eV	Area (P) CPS.eV	Atomic %
Cu2p	942.08	933.26	925.58	125500.7	2.62	391377.72	6.29
O1s	537.58	533	523.08	157488.52	3.27	552637.25	34.01
C1s	296.08	286.11	279.08	77090.97	2.97	311332.18	47.1
S2p	173.08	163.49	157.58	25725.21	1.76	87427.89	7.35
W4f	48.08	37.8	32.08	55626.81	4.11	244481.85	3.26
N1s	406.08	403.8	394.58	5371.03	3.03	21966.79	2

(a)

(b)

Figure S18. Kinetics of 0.5 mM (a) **PVMo₁₁** and (b) **PVW₁₁** reduction by 25 mM RSH under Ar. Cu(II) concentration dependence of the RSH reduction in pH = 2 H_2SO_4/Na_2SO_4 buffer.
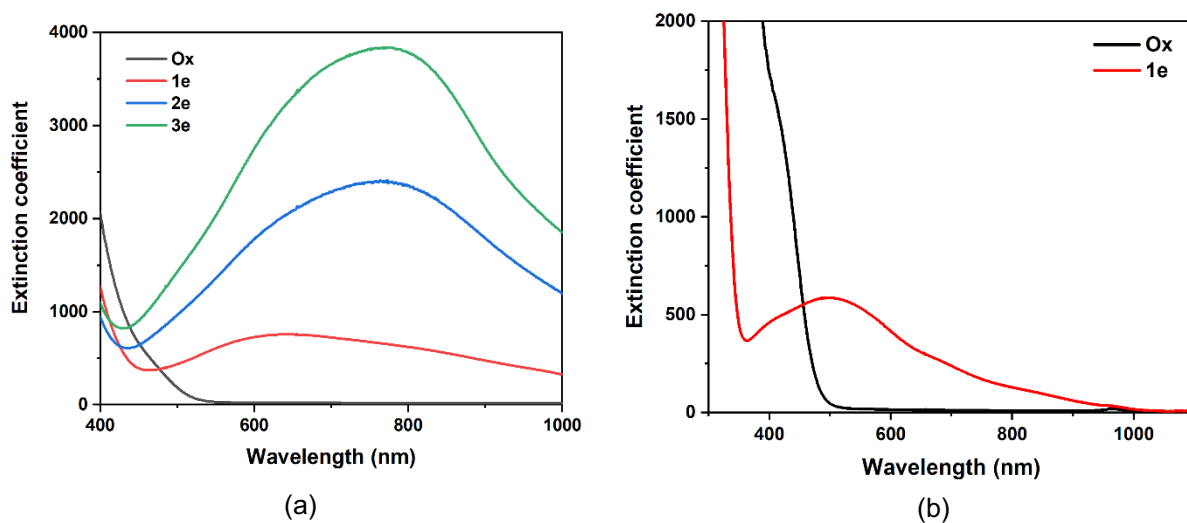

(a)

(b)

Figure S19. Bulk-electrolysis titration UV-vis spectra. (a) **PVMo₁₁**; (b) **PVW₁₁** in pH = 2 H_2SO_4/Na_2SO_4 buffer.
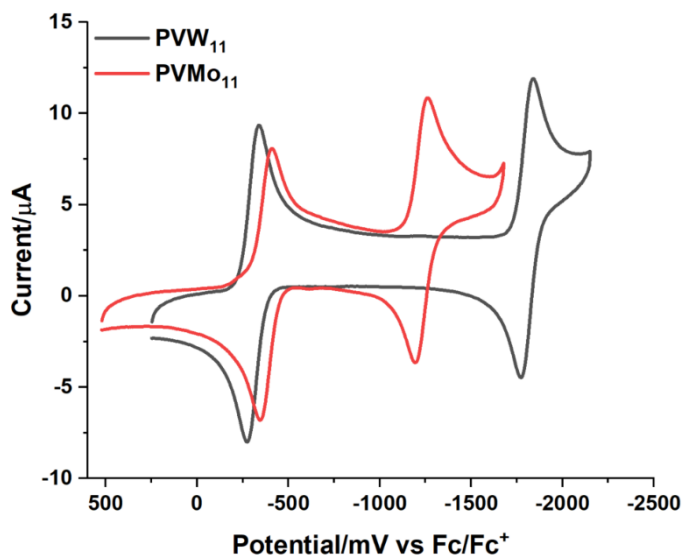
Figure S20. Black: cyclic voltammograms (CV) of 0.5 mM TBA$_4$PVMo$_{11}$O$_{40}$. Red: CV of 0.5 mM TBA$_4$PVW$_{11}$O$_{40}$. Conditions: acetonitrile, 0.1 M n-Bu$_4$NPF$_6$, scan rate = 100 mV s^{-1}, T = 298 K.

Table S4: Formal potentials (E$_{1/2}$) of V centers in the POM.

	PVW$_{11}$	PVMo$_{11}$
E$_{1/2}$^{1} (V)	-338.6	-380.3
E$_{1/2}$^{2} (Mo)	-1809.3	-1227.8

Data from Figure S20. E (mV) vs Fc/Fc$^+$

Table S5: Formal potentials (E$_{1/2}$) of V centers in the POM and POM@MOF.

	PVW$_{11}$	PVW$_{11}$@HKUST	PVMo$_{11}$	PVMo$_{11}$@HKUST
E$_{1/2}$ vs RHE	0.90	0.93	0.78	0.82

Data from Figure 9.
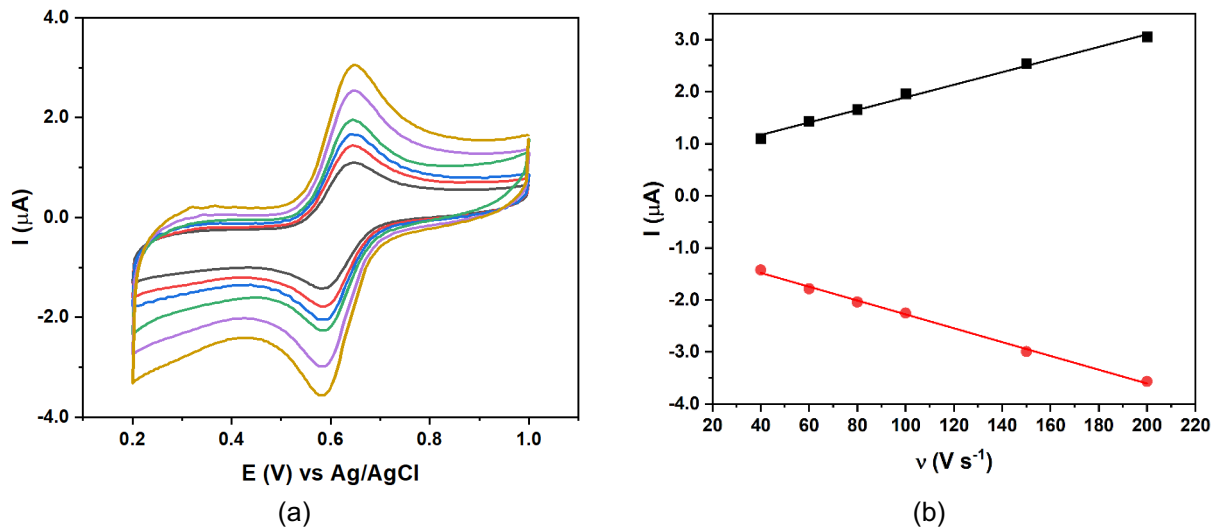
Figure S21. a) Cyclic voltammograms (CV) of **PVW$_{11}$@HKUST** immobilized on the glassy carbon (GC) electrode at different scan rate. **b)** Plots of i$_{pc}$ and i$_{pa}$ vs scan rate, v. Conditions: pH =2 H$_2$SO$_4$/Na$_2$SO$_4$ buffer, 0.1 M KNO$_3$.

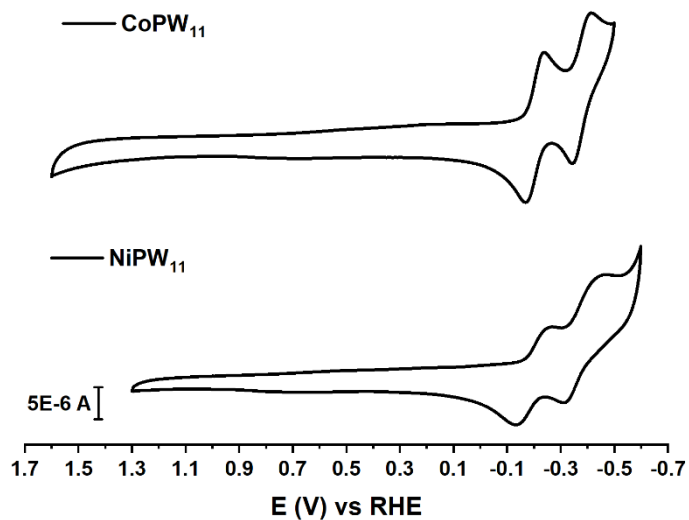**Figure S22.** Cyclic voltammograms (CVs) of 0.5 mM K$_5$PCoW$_{11}$O$_{39}$ and K$_5$PNiW$_{11}$O$_{39}$. Conditions: pH = 5 acetate buffer, 0.1 M KNO$_3$, scan rate, v = 100 mV s^{-1}, T = 298 K.
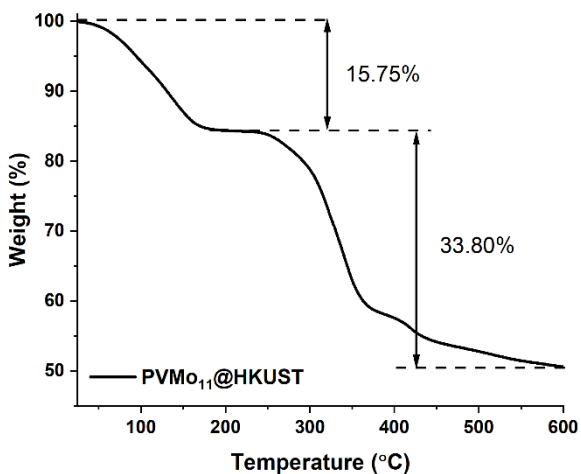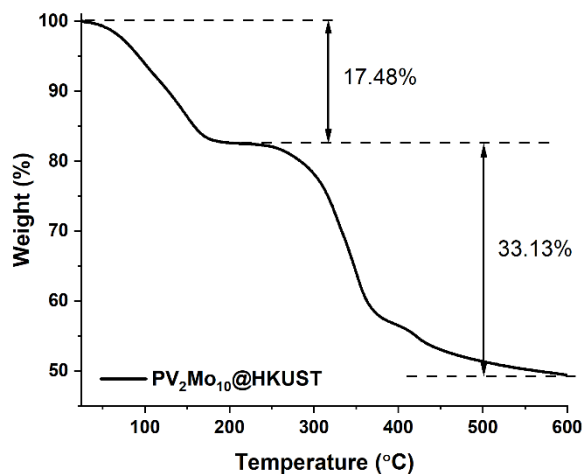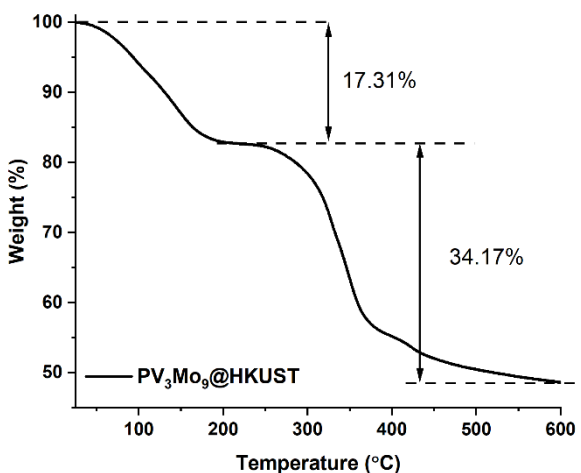
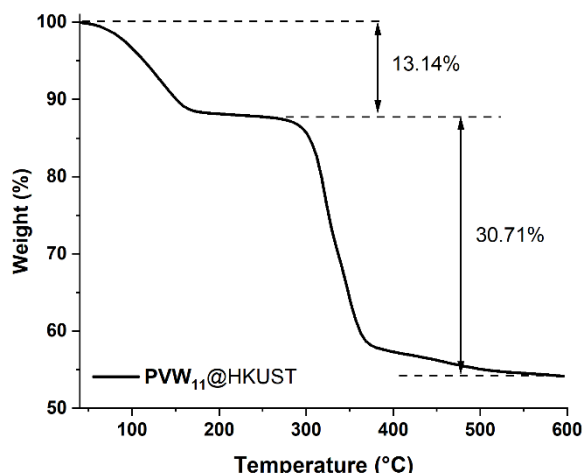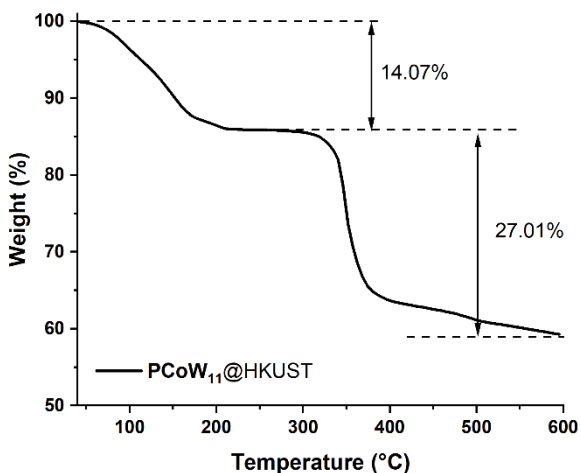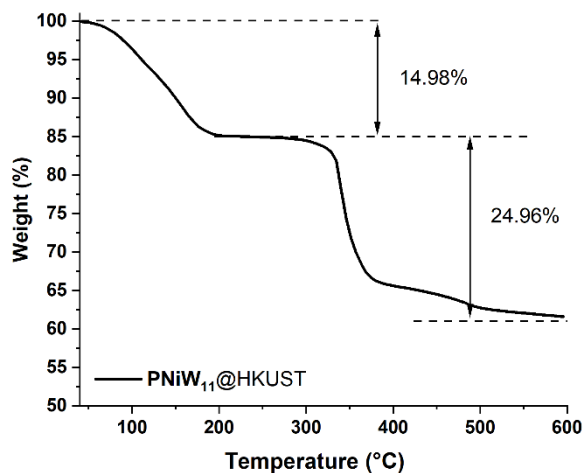**Figure S23.** Thermogravimetric analyses of the POM@MOFs. The calculated weight percentages of water + tetramethylammonium cations and the HKUST-1 framework are (a) 15.71% and 33.27% (**PVMo₁₁@HKUST**); (b) 17.39% and 32.96% (**PV₂Mo₁₀@HKUST**); (c) 17.25% and 33.57%

(**PV₃Mo₉**@HKUST); (d) 13.15% and 27.86% (**PVW₁₁**@HKUST); (e) 14.24% and 27.55% (**PCoW₁₁**@HKUST); (f) 14.17% and 27.12% (**PNiW₁₁**@HKUST), respectively, based on the empirical formula.
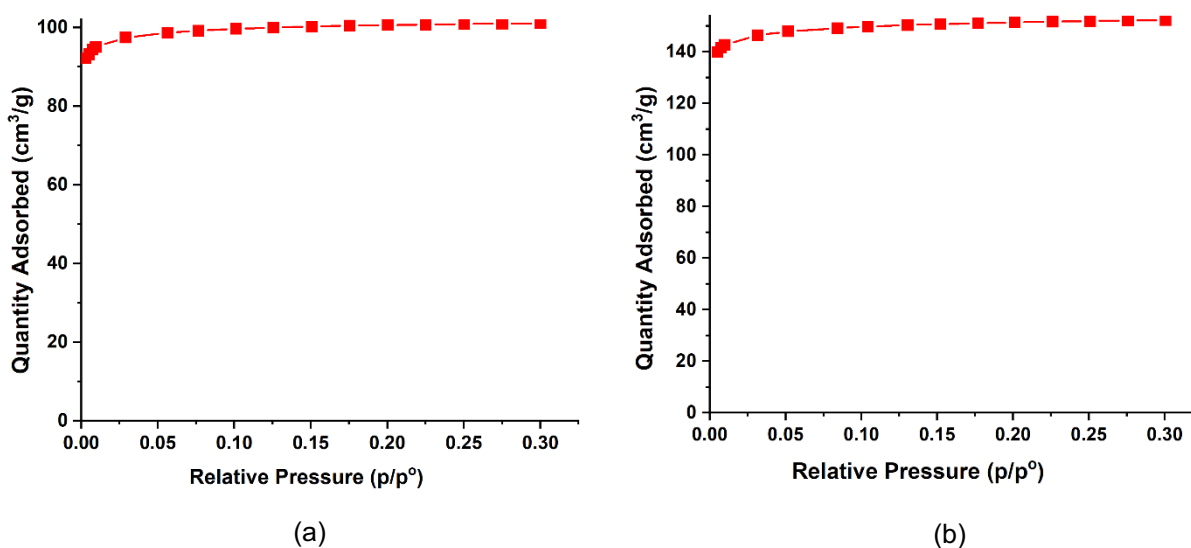

(a)

(b)

Figure S24. N₂ gas adsorption isotherms of **PV₂Mo₁₀**@HKUST and **PCoW₁₁**@HKUST measured at 77 K. The BET surface areas of **PV₂Mo₁₀**@HKUST and **PCoW₁₁**@HKUST are 619.2 and 413.5 m²/g, respectively.
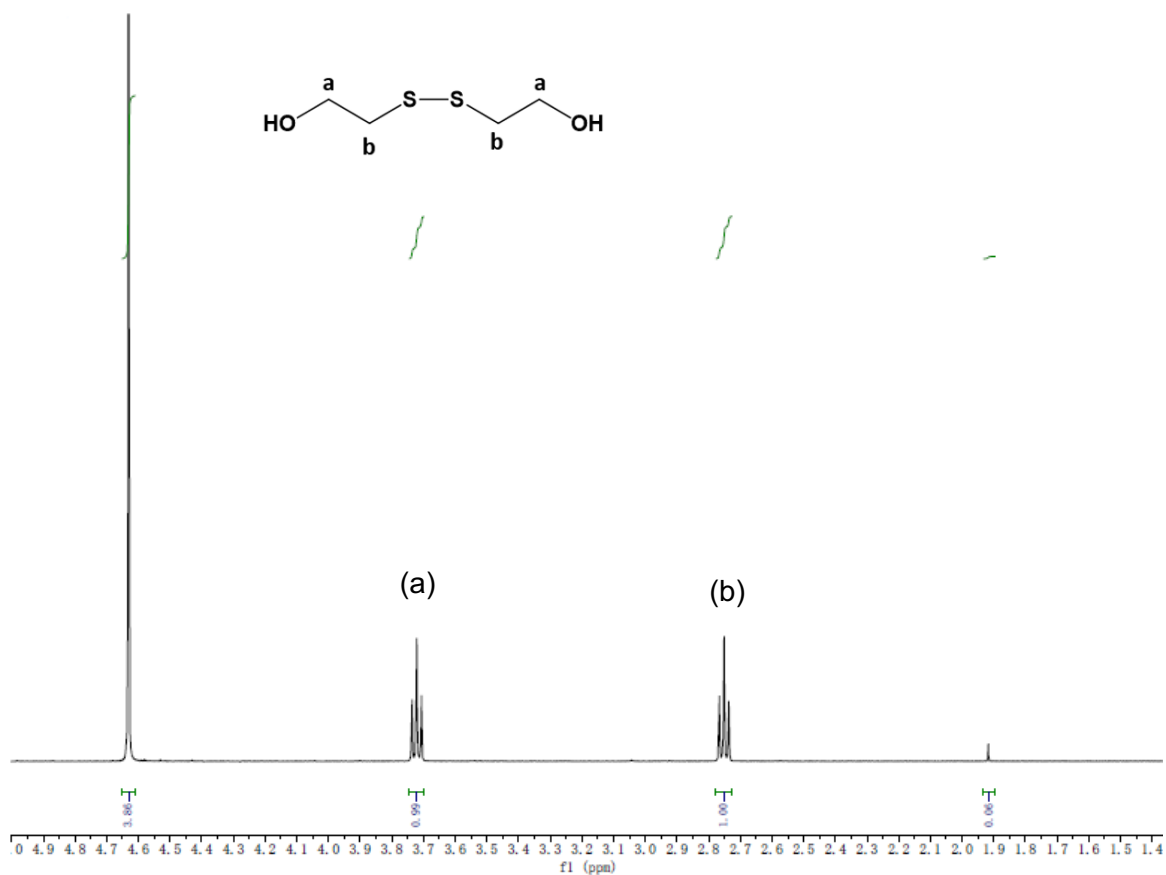
Figure S25. ^{1}H NMR spectrum at the end of the reaction. The solution was filtered to remove the solid catalyst and the solute was dissolved in deuterated H_2O.

References

1   D. P. Smith and M. T. Pope, *Inorg. Chem.*, 1973, **12**, 331–336.

2   A. G. MacDiarmid, *Inorganic Syntheses(BOOK)*, 2007, vol. 17.

3   G. A. Tsigdinos and C. J. Hallada, *Inorg. Chem.*, 1968, **7**, 437–441.

4   C. M. Tourné, G. F. Tourné, S. A. Malik and T. J. R. Weakley, *J. Inorg. Nucl. Chem.*, 1970, **32**, 3875–3890.

5   T. J. R. Weakley and S. A. Malik, *J Inorg Nucl Chem*, 1967, **29**, 2935–2944.

6   J. H. Choi, J. K. Kim, D. R. Park, T. H. Kang, J. H. Song and I. K. Song, *J. Mol. Catal. A Chem.*, 2013, **371**, 111–117.

7   H. Yang, J. Li, L. Wang, W. Dai, Y. Lv and S. Gao, *Catal. Commun.*, 2013, **35**, 101–104.

8   F. Ma, S. Liu, C. Sun, D. Liang, G. Ren and F. Wei, *J Am Chem Soc*, 2011, **133**, 4178–4187.

9   J. Song, Z. Luo, D. K. Britt, H. Furukawa, O. M. Yaghi, K. I. Hardcastle and C. L. Hill, *J. Am. Chem. Soc.*, 2011, **133**, 16839–16846.

10   L. Bromberg, Y. Diao, H. Wu, S. A. Speakman and T. A. Hatton, *Chem. Mater.*, 2012, **24**, 1664–1675.

11   B. Botar, Y. V. Geletii, P. Kögerler, D. G. Musaev, K. Morokuma, I. A. Weinstock and C. L. Hill, *J. Am. Chem. Soc.*, 2006, **128**, 11268–11277.

12   X. Lu, T. Cheng, Y. V. Geletii and C. L. Hill, *Inorg. Chem.*, 2023, **5**, 2404–2414.